Validation of an Erythema-Weighted UV Model Using Broadband Solar Irradiance Measurements From Eleven U.S. Sites

Agustín Laguarda[1], Aron Habte[2], Gonzalo Abal[1], and Manajit Sengupta[2]

[1] Laboratorio de Energía Solar/Universidad de la República, Montevideo (Uruguay)

[2] National Renewable Energy Laboratory, Colorado (USA)

Abstract

Erythema-weighted UV solar irradiance (UV-E) has a potential impact on human health if the recommended maximum exposure times are exceeded. In spite of this, it is not measured at most sites that measure Global Horizontal Irradiance (GHI). However, since UV-E is highly correlated with GHI and total ozone content it can be estimated from this information with sufficient accuracy to assisst in public health recommendations. The Power Model (PM) provides a simple method to estimate the erythema-weighted UV irradiance (UV-E) from measured GHI, total ozone column and air mass. In this work, the performance of the PM method is assessed using high-quality data from 11 sites in the continental U.S. (part of SURFRAD and SOLRAD networks) and total ozone estimates publicly available from the MERRA-2 re-analysis database. A three year period (2021-2023) at 1-minute frequency is considered. The results (for time aggregations of 5 and 60 minutes) show a high Pearson's correlations (> 0.99), consistently positive mean bias deviations (below 13%) and dispersions in the 8-19% range at all sites. Relative values are expressed in terms of the corresponding measurement mean. The performance indicators remain consistent across time resolutions (5 or 60 minutes), suggesting that the model's performance is robust and not significantly affected by short-term variability (which is captured by GHI). Spatial patterns reveal higher biases and RMSD in northern and eastern locations. These values represent a significant improvement over widely used satellite-based global UV-E estimates and open the possibility of using the PM with satellite-based GHI estimates for operational UV-E mapping over the contiguous U.S. territory.

Keywords: solar modeling, UV irradiance, empirical model, erythema-weighted UV, quality assessment

1. Introduction

Ultraviolet-B (UV-B) radiation, particularly in its erythema-weighted form (UV-E), impacts the material degradation of polymers, encapsulants in photovoltaic modules, and human health. Although direct UV-E measurements provide the most accurate ground-level exposure assessments, they are limited in spatial and temporal coverage due to the high costs and maintenance demands of UV radiometers, which require re-calibration at one year periods. Alternatively, satellite-based products, such as the Copernicus Atmosphere Monitoring Service (CAMS) and the European Centre for Medium-Range Weather Forecasts ultraviolet product (ECMWF-UV), offer broader regional estimates; however, their accuracy often exhibits relative root mean square deviations (rRMSD) of 30%–40% and mean biases up to ±20% (Pitkänen et al., 2020) of the measurements' mean.

Alternative modeling approaches include radiative transfer simulations, machine learning, and empirical models. Among these, phenomenological models based on widely available inputs—such as global horizontal irradiance (GHI), relative air mass, and total column ozone—offer a fast and efficient method for estimating UV-E. Notably, the Power Model (PM), introduced by Antón Martínez (2009) and further improved and extensively evaluated in recent studies (Laguarda et al. 2019; 2024; 2025), defines the UV-E fraction through power functions of clearness index, air mass, and ozone levels. The PM has demonstrated strong performance

at 10-minute resolution using ground data from five midlatitude sites in the Americas, achieving relative errors below 12% and low bias, particularly under clear-sky and low-air-mass conditions (Laguarda et al., 2024).

The current study evaluates the PM's performance at 5-minute and 60-minute resolutions with high-quality UV and GHI data from seveal U.S. sites, which span diverse geographic and climatic conditions. These sites were not were not used in the PM's development or calibration, thus providing an independent validation framework. Further, the new dataset enables a comprehensive assessment of the PM's robustness and limitations under operational conditions.

2. Data Used

2.1 Ground Measurements

The evaluation presented here is based on data from 11 sites distributed across the continental United States, with latitudes ranging from 35° to 49° and encompassing a variety of elevations and Köppen-Geiger (Peel et al. 2007) climate regions (see Table 1 and Figure 1). These sites, which provide 1-minute frequency measurements of solar radiation components, belong to two well-established networks: the Surface Radiation Budget Network (SURFRAD) and the Solar Radiation Monitoring Station Network (SOLRAD) (Augustine et al., 2005).[1] Both networks are currently operated and maintained by the National Oceanic and Atmospheric Administration (NOAA). The analysis uses a common time span of 3 years (from 2021 to 2023) for all sites, with further data aggregation at 5 and 60-minute time resolutions.

Table 1. Site location, elevation, data provider, and Köppen-Geiger climate classification

Code	Location	Latitude (North)	Longitude (West)	Elevation (meters)	Climate clasification	Network
ABQ	Albuquerque, New Mexico	35.04	106.62	1617	BSk	SOLRAD
BIS	Bismark, North Dakota	46.77	100.76	503	Dfb	SOLRAD
HNX	Hanford, California	36.31	119.63	73	BSk	SOLRAD
SLC	Salt Lake City, Utah	40.77	111.96	1288	Csa/Dsa	SOLRAD
STE	Sterling, Virginia	38.97	77.49	85	Cfa	SOLRAD
BON	Bondville, Illinois	40.05	88.37	213	Dfa	SURFRAD
DRA	Desert Rock, Nevada	36.62	116.02	1007	Bwh	SURFRAD
FPK	Fort Peck, Montana	48.31	105.10	634	BSk	SURFRAD
PSU	Penn State, Pennsylvania	40.72	77.93	376	Dfb	SURFRAD
SXF	Sioux Falls, South Dakota	43.73	96.62	473	Dfa	SURFRAD
TBL	Table Mountain, Colorado	40.13	105.24	1689	Dfc	SURFRAD

[1]SOLRAD: https://gml.noaa.gov/grad/solrad/, SURFRAD: https://gml.noaa.gov/grad/surfrad/, accesed in September 2024.

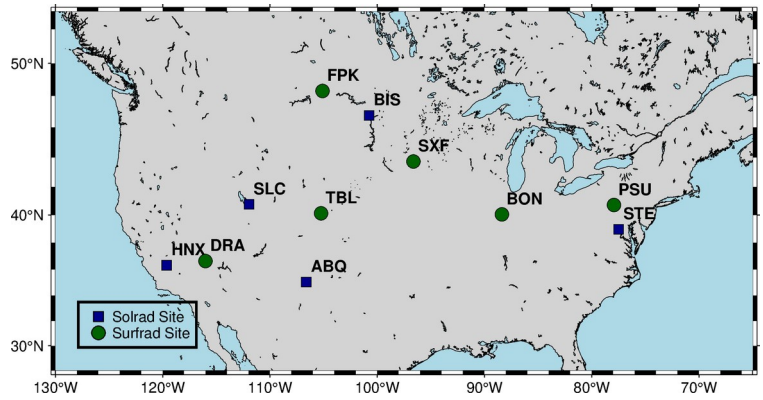

Figure 1. Sites from the SOLRAD and SURFRAD networks considered in this work

2.2 Ozone Information

Total column ozone data were retrieved from the Modern-Era Retrospective analysis for Research and Applications, Version 2 (MERRA-2) reanalysis dataset (Gelaro et al., 2017), produced by the National Aeronautics and Space Administration's (NASA's) Global Modeling and Assimilation Office (GMAO). MERRA-2 provides globally gridded atmospheric data with a spatial resolution of 0.5° latitude × 0.625° longitude and a temporal resolution of 1 hour, making it suitable for capturing diurnal ozone variability. For this study, the total column ozone values were temporally interpolated to match the 5-minute resolution of the surface irradiance measurements. This ozone information was then used as input to the PM to account for the absorption effects of stratospheric ozone on UV-E irradiance.

3. Methodology

3.1 Power Model Description

The PM, proposed in Laguarda (2019, 2024), is an empirical parametrization for estimating UV-E fraction, f_{UV} = UV-E/GHI. It relies exclusively on three predictors: the clearness index (k_t), the total ozone column (TOC, in DU) and the relative air mass (m). The clearness index is the GHI normalized by the incident horizontal irradiance at the Top of the Atmosphere (TOA). For our purposes, where low-Sun records are excluded, the relative air mass m can be approximated with sufficient accuracy as 1/cos z, in terms of the solar zenith angle z. The PM expresses the UV-E fraction as:

$$f_{UV} = a_0 \cdot k_t^{\,a_1} \cdot m^{a_2} \cdot \left(\frac{TOC}{100}\right)^{a_3} \qquad \text{(eq. 1)}$$

The coefficients were previously determined using data from five midlatitude sites in the United States and South America and were found to be fairly robust across sites (Laguarda et al., 2024). In this work, the model is applied using the average coefficients derived in that study: a_0=0.705, a_1=-0.207, a_2=-1.247, and a_3=-0.950.

3.2 Data Processing

In all sites, simultaneous GHI and UV-E measurements were originally registered at 1-minute intervals. A quality assessment (QA) procedure was applied, beginning with the exclusion of data for solar altitudes below 10° (i.e., cosine of the solar zenith angle, cos(z) < 0.174) and followed by the three filters:

F1: $0 \le GHI \le 50 + I_0 \cdot \left(\cos\left(z\right)\right)^{1.1}$ (Long and Shi, 2008)

F2: $0 \le UVE \le 10 + 350 \cdot \left(\cos\left(z\right)\right)^{2.2}$ (Laguarda, 2024)

F3: $0.18 \times \left(\cos\left(z\right)\right)^2 \le f_{UV} \le 0.2 \times \left[1 + \left(\cos\left(z\right)\right)^2\right]$ (Laguarda, 2024)

where I_o is the mean extraterrestrial solar irradiance (1361 W/m^2) corrected for the Earth-Sun distance, GHI is in W/m^2, and UVE is in mW/m^2. The F1 filter is based on the QA procedure recommended by the Baseline Surface Radiation Network (BSRN, Long and Shi, 2018), while the F2 and F3 filters were proposed in Laguarda et al. (2024). Figure 2 illustrates the application of the F2 and F3 filters for the TBL site as an example, highlighting the effect of each criterion on the 1-minute dataset. Table 2 summarizes the results of the QA procedure. Across all sites, between 80.2% and 86.7% of the initially diurnal valid data were retained after filtering. The solar altitude criterion was the most limiting factor, contributing to more than 15% of the overall data rejection.

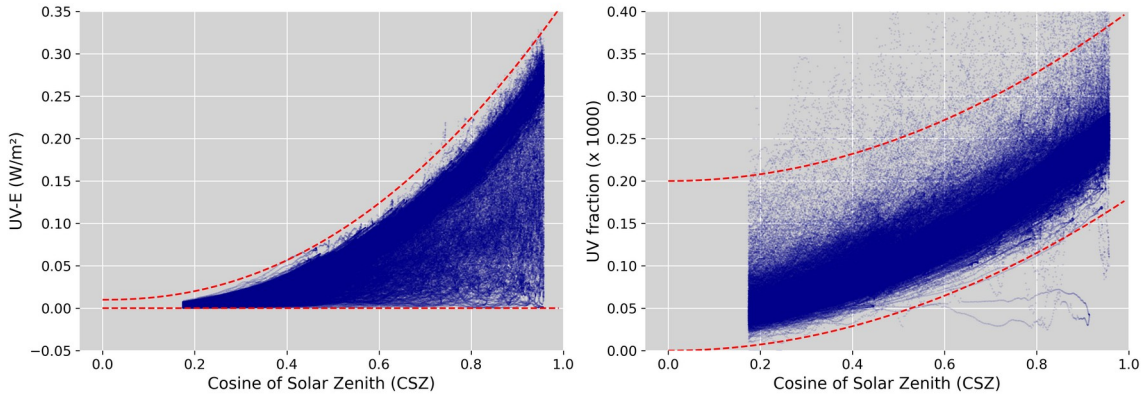

Figure 2. Effect of the F2 filter (left) and F3 filter (right) on the 1-minute dataset for TBL. Blue points correspond to data with solar altitudes greater than 10° that also passed the F1 filter. Dashed red lines indicate the thresholds applied for F2 and F3, respectively.

Table 2. Number of existing diurnal 1-minute records and percentage of data retained at each stage of the QA procedure for each site. The top row shows the total number of diurnal records initially considered (100%). The final row indicates the proportion of data retained after all the QA filters, relative to the initial valid dataset.

	BON	DRA	FPK	PSU	SXF	TBL	ABQ	BIS	HNX	SLC	STE
Valid data	783195	791745	770183	783130	782050	779397	736365	615810	766988	781060	793143
CSZ > 0.174	83.8	84.4	81.1	83.4	82.6	84.2	85.4	81.4	86.7	84.4	84.1
F1	83.8	84.3	81.0	83.3	82.5	83.9	85.2	81.3	86.7	84.3	84.1
F1 & F2	83.8	84.3	81.0	83.3	82.5	83.9	85.2	81.3	86.7	84.3	84.1
F1&F2&F3	83.2	83.8	80.2	82.5	82.0	83.2	84.4	80.7	86.0	83.7	83.1

Following the QA, all data were aggregated to 5-minute intervals to match the temporal resolution of the satellite-derived GHI estimates from the Geostationary Operational Environmental Satellite (GOES) series, which operates at a native 5-minute cadence over North America. Aggregation was performed only when at least four 1-minute records within each 5-minute window passed all QA filters, ensuring the representativeness of the resulting averages. Although additional evaluations were conducted at 10-, 30-, and 60-minute resolutions (aggregating only when at least four of five 1-minute records were valid), performance

improvements were minor; therefore, only the 60-minute results are retained for comparison with the 5-minute baseline. In this study, UV-E irradiance at a 5-minute resolution is considered the reference (ground truth), whereas the ground-measured GHI is used to compute the clearness index k_t (Eq. 1) and serve as an input for the UV estimation.

3.3 Performance Indicators

The model performance was assessed using standard statistical indicators: the mean bias deviation (MBD), the root mean square deviation (RMSD), and the Kolmogorov-Smirnov integral (KSI). The MBD represents the average deviation between the model estimates and observations, indicating systematic bias; and the RMSD quantifies the dispersion of residuals, capturing both bias and other errors. Additionally, the KSI provides a statistical similarity measure by integrating the absolute difference between the empirical cumulative distribution functions estimated from the modeled and observed values , (Massey, 1951; Espinar et al., 2009). To facilitate comparison across sites with different irradiance levels, the metrics are expressed in relative terms as as percentages of the mean of the observed UV-E irradiance (in mW/m^2) (rMBD, rRMSD, rKSI).

4. Results

4.1 Overall Performance of the Model

The results of the model assessment at a 5-minute frequency are summarized in Table 3. The model exhibits strong agreement across all sites, with the Pearson correlation values consistently ranging between 0.990 and 0.996 (not shown in the Table 3). The rMBD is consistently positive, indicating an overestimation of UV, except for the ABQ site, which shows a slight negative rMBD. The highest rMBD is found at STE (12.5%), whereas the lowest occurs at DRA (2.7%).

Table 3. Relative metrics and relevant data for each site at 5-min resolution. All metrics are expressed as % of the mean value of the measurements (last row) which is in mW/m2.

	BON	**DRA**	**FPK**	**PSU**	**SXF**	**TBL**	**ABQ**	**BIS**	**HNX**	**SLC**	**STE**
rMBD (%)	10.6	2.7	9.1	10.0	7.5	3.6	-0.1	9.4	9.5	5.3	12.5
rRMSD (%)	16.7	8.4	18.5	16.9	15.7	11.0	8.5	18.2	13.3	11.7	18.8
rKSI (%)	4.8	2.9	4.4	4.3	3.8	2.5	2.7	3.7	5.8	2.9	5.7
Data pairs	129439	132010	122825	128479	127669	128921	123536	98855	131370	129943	130973
Mean (mW/m^2)	57.4	88.1	52.0	53.7	56.9	69.89	94.8	50.1	79.7	69.3	57.9

The rRMSD is in the range 8.4% to 18.8%, with the lowestvalue observed at DRA and the highest at STE. The rKSI ranges between 2.7% and 5.8%, also confirming a good agreement between the distribution of the observed and estimated values. Note that lower relative errors (rMBD and rRMSD) are often observed at sites with a higher mean UV-E irradiance, such as ABQ and DRA. This pattern is partly due to the fact that dry, sunny sites (such as DRA, HNX or ABQ) tend to exhibit higher mean values and correspondingly lower relative error metrics. Additionally, the reduced prevalence of cloudiness in these regions reduces the variability in the data, which favors the accuracy of the model.

Figure 3 shows the spatial distribution of the rMBD and rRMSD across all sites. The rMBD is represented by the color scale, with higher values observed at the northern and eastern sites (e.g., FPK, BIS, PSU, STE). Minimum biases occur in the southwest (e.g., ABQ, DRA), where clear-sky conditions are more frequent. The rRMSD, shown by the size of the circles, follows a similar distribution, suggesting that both systematic and other errors are influenced by regional atmospheric characteristics.

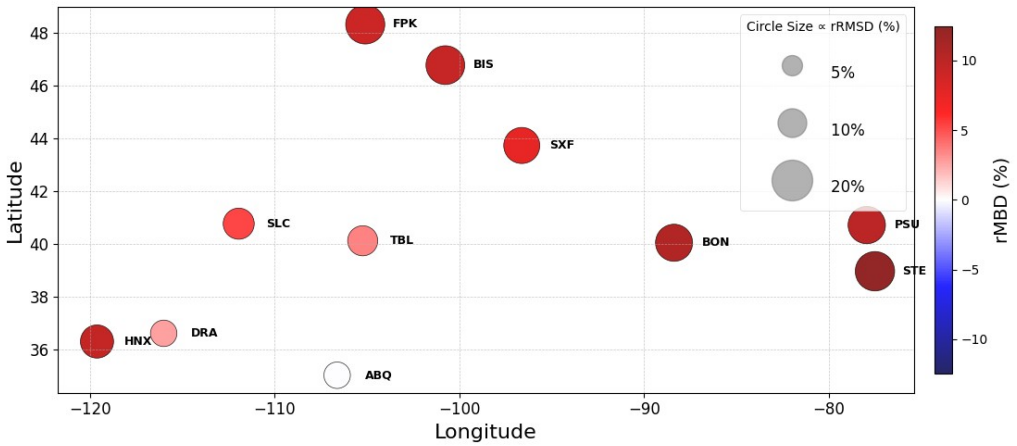

Figure 3. Spatial distribution of rMBD (color of the cirlces) and rRMSD (radius of the cirlces) across sites

Figure 4 presents the variation of rMBD and rRMSD at different temporal aggregations. On average, the bias and the rKSI (not shown) are virtually the same, and the rRMSD changes by 0.2% (average across sites) between the 5-minute and 60-minute resolutions. Although increasing the aggregation period typically maintains the bias and reduces variability, thus potentially improving the model performance, this effect is not evident here. These results suggest that the model performs equally well at both temporal resolutions.

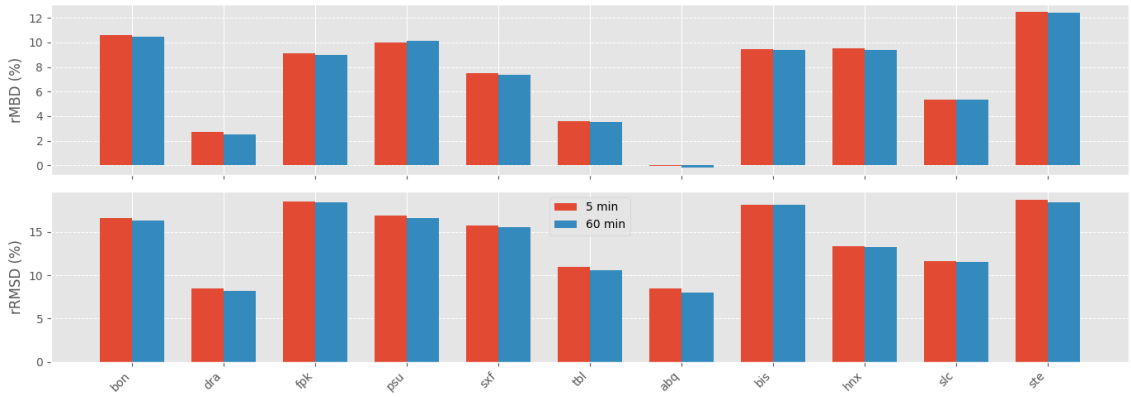

Figure 4. Variation of selected model performance metrics (rMBD and rRMSD) as a function of temporal resolution (5 minute vs. 60 minute) across all sites.

Finally, in Figure 5, the scatter plots of the PM versus measurements are presented for TBL for the two time resolutions considered here. The agreement is strong for the two cases, as highlighted by the accumulation of points around the y = x curve, where the color is clearer.

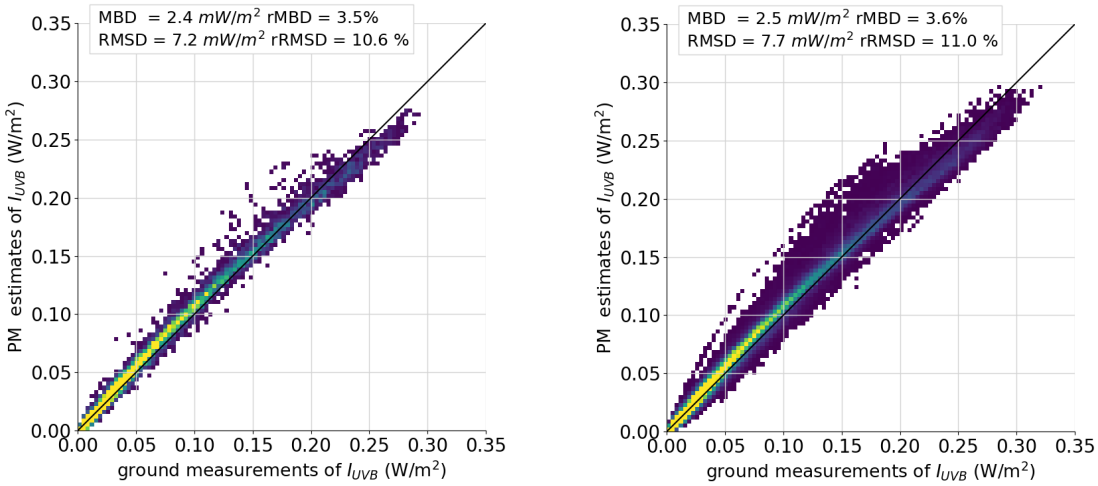

Figure 5. Scatter plots of estimated versus observed UV-E irradiance at the TBL site for 5-minute and 60-minute resolutions. Point density is indicated by color, with yellow regions representing areas of higher data concentration.

5. Conclusions

The usefulness of the Erithema-weighted UV estimates obtained from the PM method driven by high-quality ground data and MERRA-2 total ozone estimates has been established. These estimates represent a significant improvement over currently used satellite based estimates of UV-E with global coverage. In an empirical model such as the PM, some noticeable mean biases are anticipated because it relies on average coefficients; however, the biases identified in this study are mostly less than 10% across various sites, which is a plausible range for the model's intended use.

Model performance is consistent across different temporal resolutions, with comparable accuracy at both 5-minute and 60-minute aggregations. This indicates robustness in the estimation method regardless of short-term variability.

Further analysis of cloud regimes and their influence on model performance might help explain site-specific deviations, especially in high-bias locations, such as FPK and PSU. Additionally, a specific evaluation in the northern and eastern sites (e.g., BIS, FPK, PSU, STE) is required to validate the model's applicability under diverse climatic conditions and to confirm its robustness across regions.

This study represents an initial step toward adapting the model for use with satellite-based GHI data from the National Solar Radiation Database (NSRDB) to enable broader UV estimation across continental scales.

6. Acknowledgments

The authors acknowledge NASA's GMAO for providing the MERRA-2 reanalysis data used in this study. Thanks are also expressed to the several technicians and experts who collected and curated the data from the SOLRAD and SURFRAD networks. A. L. and G. A. would like to express their gratitude to the Universidad de la República (Udelar) for its continued support and acknowledge the Comisión Sectorial de Investigación Científica (CSIC) for its support through the CSIC Grupos program. A. L. also acknowledges the Programa Despegue Científico of PEDECIBA for additional support.

This work was authored in part by NREL for the U.S. Department of Energy (DOE), operated under Contract No. DE-AC36-08GO28308. Funding for the NREL authors provided by U.S. Department of Energy Office of

Energy Efficiency and Renewable Energy Solar Energy Technologies Office. The views expressed in the article do not necessarily represent the views of the DOE or the U.S. Government. The U.S. Government retains and the publisher, by accepting the article for publication, acknowledges that the U.S. Government retains a nonexclusive, paid-up, irrevocable, worldwide license to publish or reproduce the published form of this work, or allow others to do so, for U.S. Government purposes.

7. References

Antón, M., Serrano, A., Cancillo, M. L., and García, J. A. (2009). An empirical model to estimate ultraviolet erythemal transmissivity, Ann. Geophys., 27, 1387-1398, https://doi.org/10.5194/angeo-27-1387.

Augustine, J. A., Hodges, G. B., Cornwall, C. R., Michalsky, J. J., Medina, C. I., 2005. An update on SURFRAD-The GCOS Surface Radiation Budget Network for the continental United States. Journal of Atmospheric and Oceanic. Technology 22, 1460-1472.

Espinar, B., Ramírez, L., Drews, A., Beyer, H.G., Zarzalejo, L.F., Polo, J., Martín, L., (2009). Analysis of different comparison parameters applied to solar radiation data from satellite and German radiometric stations. Solar Energy 83, 118–125.

Gelaro, R., McCarty, W., Suárez, M., Todling, R., Molod, A., Takacs, L., Randles, C., Darmenov, A., Bosilovich, M., Reichle, R., y Wargan, K. (2017). The Modern-Era Retrospective Analysis for Research and Applications, Version 2 (MERRA-2). Journal of Climate, 30: 5419–5454.

Long, C. y Shi, Y. (2008). An automated quality assessment and control algorithm for surface radiation measurements. The Open Atmospheric Science Journal, 2:23-37.

Laguarda, A. and Abal, G., 2019, Assessment of empirical models to estimate UV-A, UV-B and UV-E solar irradiance from GHI. Proc.ISES-SWC, Chile, 4–7, 2019, https://doi.org/10.18086/swc.2019.42.04.

Laguarda, A., Abal, G., 2025. UV Index from Global Solar Irradiance: Performance according to cloudiness and air mass. *Air Qual Atmos Health* **18**, 2687–2703 (2025). https://doi.org/10.1007/s11869-025-01788-3

Laguarda, A., Abal, G., Russo, P., and Habte, A. (September 4, 2024). "Estimating UV-B, UV-Erithemic, and UV-A Irradiances From Global Horizontal Irradiance and MERRA-2 Ozone Column Information." ASME. *J. Sol. Energy Eng*. April 2025; 147(2): 021001. https://doi.org/10.1115/1.4066202

Massey, F. J. (1951). The Kolmogorov-Smirnov Test for Goodness of Fit. *Journal of the American Statistical Association*, *46*(253), 68–78. https://doi.org/10.1080/01621459.1951.10500769.

Peel, M. C., Finlayson, B. L., Mcmahon, T. A., 2007. Updated world map of the Köppen-Geiger climate classification. Hydrology and Earth System Sciences Discussions 11, 1633–1644.

Pitkänen M, Wandji W, Arola A., (2020). Validation report of the CAMS UV processor. Tech. Rep. 19, Copernicus Atmosphere Monitoring Service, URL https://atmosphere.copernicus.eu/sites/default/files/2020-11/19_CAMS72_2018SC2_D72.2.1.1-2020Q3_UV_VAL_202009_v1.pdf